Coexistence of Competing Orders with Two Energy Gaps in Real and Momentum Space in the High Temperature Superconductor $Bi_2Sr_{2-x}La_xCuO_{6+\delta}$

J.-H. Ma,[1] Z.-H. Pan,[1] F. C. Niestemski,[1] M. Neupane,[1] Y.-M. Xu,[1] P. Richard,[1,2] K. Nakayama,[3] T. Sato,[3] T. Takahashi,[2,3] H.-Q. Luo,[4] L. Fang,[4] H.-H. Wen,[4] Ziqiang Wang,[1] H. Ding,[1,4] and V. Madhavan[1]

[1]*Department of Physics, Boston College, Chestnut Hill, Massachusetts 02467, USA*
[2]*WPI Advanced Institute for Materials Research, Tohoku University, Sendai 980-8577, Japan*
[3]*Department of Physics, Tohoku University, Sendai 980-8578, Japan*
[4]*Institute of Physics and National Laboratory for Condensed Matter Physics, P. O. Box 603 Beijing, 100080, People's Republic of China*

(Received 22 July 2008; published 13 November 2008)

Through a combined scanning tunneling microscopy and angle-resolved photoemission spectroscopy study, we report the observation of two distinct gaps (a small and a large gap) that coexist both in real space and in the antinodal region of momentum space, below the superconducting transition temperature (T_c) of $Bi_2Sr_{2-x}La_xCuO_{6+\delta}$. We show that the small gap is associated with superconductivity. The large-gap persists above T_c, and seems linked to observed charge ordering. We find a strong correlation between the large and small gaps suggesting that they are affected by similar physical processes.

DOI: 10.1103/PhysRevLett.101.207002 PACS numbers: 74.25.Jb, 74.20.−z, 74.62.−c, 74.72.Hs

The crux of the intense debate on the pseudogap phase [1,2] revolves around the issue of whether it is a precursor pairing state without superconducting coherence or a competing phase with a hidden order parameter. Many earlier experimental results on the pseudogap demonstrated characteristics of a precursor pairing gap, including similar gap amplitudes and d-wave-like momentum dependence above and below T_c, and smooth temperature evolution through T_c [3]. This has led to the belief that the superconducting phase is characterized by a single d-wave pairing order parameter which also finds support in the observation of a single d-wave gap function in cases where the Bogoliubov quasiparticle peak survives at the antinode [4]. Recently, there has been increasing evidence for the existence of two distinct gaps associated with different order parameters coexisting below T_c, such as deviations from a single d-wave gap function [5,6], opposite doping dependence for the two gaps [7,8], and different temperature dependences of the two gaps [4,5,9] all of which suggest a competing order explanation for the pseudogap phase.

In this paper we report a detailed study of lanthanum substituted $Bi_2Sr_{2-x}La_xCuO_{6+\delta}$ (La-Bi2201), using scanning tunneling microscopy (STM) and angle-resolved photoemission spectroscopy (ARPES). These complementary data sets on identical samples (from the same batch) provide important new information that cannot be obtained from one technique alone. STM data were obtained at 5 K on samples cleaved in UHV [10]. ARPES experiments were performed at the Synchrotron Radiation Center in Wisconsin, and at the Tohoku University ARPES lab using a microwave-driven Xenon source ($h\upsilon = 8.437$ eV) [11]. High-resolution ($E_{\mathrm{Re}} < 4$ meV, $k_{\mathrm{Re}} < 0.005$ Å^{-1}) was achieved by using this low photon energy.

We focus on two dopings: nearly optimally doped $Bi_2Sr_{1.6}La_{0.4}CuO_{6+\delta}$ (0.4La) with a T_c of 32 K and over-doped $Bi_2Sr_{1.9}La_{0.1}CuO_{6+\delta}$ (0.1La) with a T_c of 16 K. Figures 1(a), 1(d), and 1(e) show STM dI/dV spectra on 0.4La and 0.1La samples. In the 0.4La samples (the 0.1La data will be discussed later), we observe two distinct, spatially coexisting gaps at low temperatures, that we will refer to as small gap (Δ_s) and large gap (Δ_L). We observe that both Δ_s and Δ_L vary with spatial location [Fig. 1(d)]. This is illustrated statistically by a histogram of the two gaps obtained from spatial conductance maps (dI/dV maps) that shows a clear bimodal distribution of gap values [Fig. 1(c)]. The average values of Δ_s and Δ_L over maps taken in different regions are 11.4 ± 4 meV and 33 ± 10 meV.

For a comparison of real space and momentum space (k-space) data, high resolution (<4 meV) APRES data were obtained on both 0.4La and 0.1La samples. Low temperature (5 K) ARPES spectra on the 0.4La samples show an angle dependent gap [Figs. 2(a) and 2(d)] continuing smoothly into the antinodal region near (π, 0) or $\theta = 0$, albeit with suppressed quasiparticle coherence peaks. As seen in Fig. 2(d), a d-wave function fits most of the data points from the node, (π, π) or $\theta = 45°$, to the coherent arc tip (defined as the point in k-space beyond which the coherence peaks are largely suppressed). We find that the average STM small gap (11.4 meV) is comparable to the low temperature ARPES gap at the arc tip (~11 meV) [Figs. 1(b) and 1(c)]. Coupling this with our finding that the ARPES gap near the nodal region disappears above T_c allows us to associate the small STM gap with superconductivity. This immediately leads us to the question, is there a counterpart of the STM large gap in ARPES?

Earlier ARPES experiments on similar samples (Pb-La-Bi2201) found a large antinodal gap of about 35 meV both above and below T_c [6], similar in magnitude to our STM

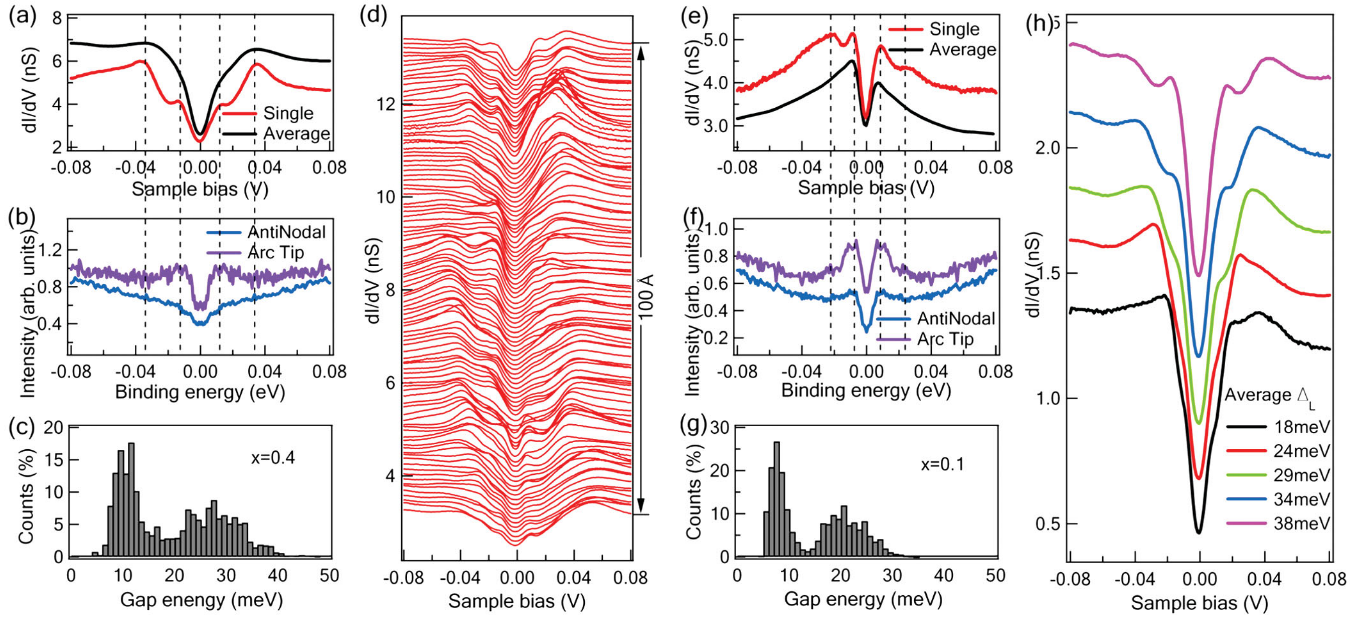

FIG. 1 (color). (a) Single STM spectrum (red) representative of the average Δ_s and Δ_L and a spatially averaged STM spectrum (black) from a 240 Å dI/dV map. (a),(b),(c),(d) and (h) show data on 0.4La samples. (b) Symmetrized ARPES energy distribution curves (EDCs) taken at antinodal position and at the arc tip ($\theta \sim 21°$) (see inset to Fig. 2(d) for definition of θ). (c) Gap histogram (237 Å dI/dV map) with average Δ_s at 10.50 meV $\pm$ 2.8 meV and Δ_L average at 27.2 meV $\pm$ 5.4 meV. (d) Spectra along a 100 Å line. (e),(f), and (g) Similar data as (a),(b), and (c) but for the 0.1La samples. Arc tip angle $\theta \sim 18°$. Average Δ_s is 7.4 meV $\pm$ 1.6 meV and average Δ_L is 20.7 meV $\pm$ 3.9 meV. (h) Spectra from a 240 Å map sorted and averaged on the basis of Δ_L.

large gap. Thus, one could invoke the idea that there are two gaps which coexist spatially but occupy different regions of momentum space [solid lines in Fig. 2(f)]. Within this picture, the large gap would be responsible for truncating the antinodal part of the Fermi surface and producing the Fermi arc in the normal state pseudogap phase, while pairing below T_c is restricted to the Fermi arc. Remarkably, we find that this picture may be incorrect. Our low photon energy, high-resolution ARPES enhances the features of the coherent excitations such that even data near the antinodal region reveal smaller gaps (maximum gap $\sim$14 meV) which follow the d-wave fit reasonably

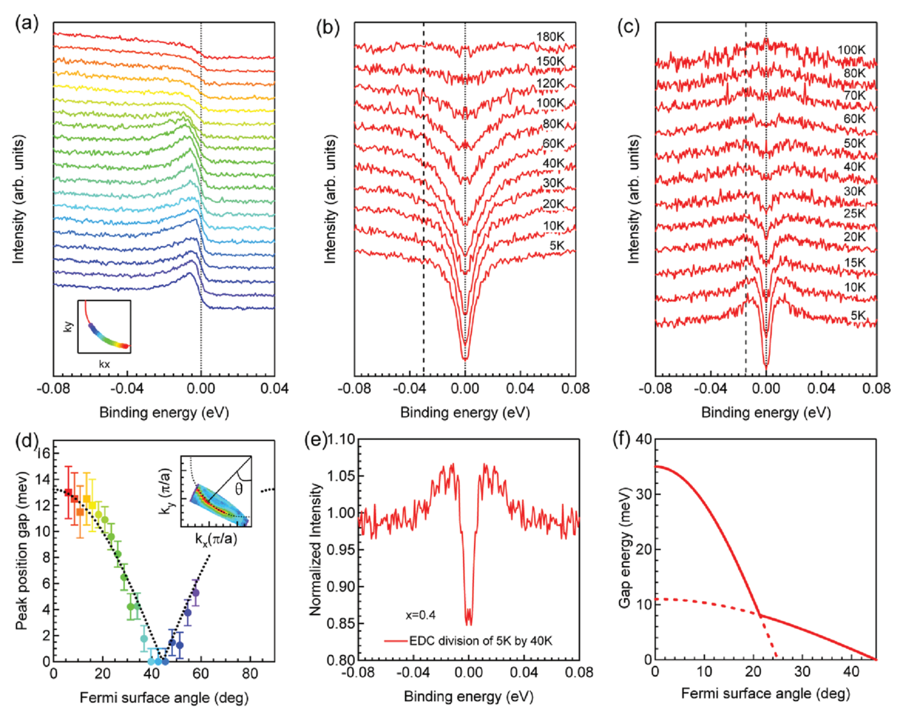

FIG. 2 (color). (a) ARPES spectra showing momentum (k) dependence of EDCs of 0.4La sample. (b) Temperature dependence of symmetrized EDCs for 0.4La sample at antinode. Dotted line is a guide to the eye to show the large pseudogap above T_c. (c) Same as (b) for 0.1La sample (d) k-dependent gap value Vs Fermi surface angle (defined in the inset) for data shown in (a), extracted by locating the coherence peak position (dots), a feasible method only up to the coherence arc tip, and by the position of the slope change thereafter (squares). (e) Division of antinodal 5 K EDC by 40 K EDC for 0.4La sample reveals coherence peaks that mask the larger gap. (f) Schematic of gap Vs angle showing the previously proposed two gap picture (solid lines) and our new proposal (solid plus dotted lines) based on the STM and ARPES data.

well [Fig. 2(d)]. This indicates a superconducting gap persisting to the antinodes, consistent with recent data on optimally doped (34 K) La-Bi2201 [12]. The observed "pairing beyond the Fermi arc" can be explained by the fact that the large pseudogap near the antinodes [1,6] is a soft gap with suppressed but finite in-gap density of states that could facilitate pairing below T_c.

The above discussion suggests that the various experimental data can be reconciled within a scenario where the small and large gaps coexist in the antinodal region [13]. The large gap near the antinode is not clearly visible in our low temperatures ARPES spectra since the spectral weight associated with the superconducting coherence masks the signal from the large gap. Accordingly, we expect it to come to the forefront after the coherence peaks disappear above T_c. Indeed, this is precisely what we observe. ARPES antinodal spectra at higher temperatures show a distinctly larger pseudogap which eventually disappears at approximately 180 K, as shown in Fig. 2(b). Based on our data the two gaps remain distinct and do not merge into one "quadrature" gap, ($\Delta = \sqrt{\Delta_s^2 + \Delta_l^2}$). Instead, our data are consistent with a new picture (explored theoretically only recently [14,15]) where below T_c, the superconducting gap persists beyond the arc tip all the way to the antinode [dotted lines in Fig. 2(f)].

STM and ARPES on the overdoped 0.1La samples take us a step further in our understanding. ARPES data at 5 K [Figs. 1(f) and 2(c)] reveal that coherence peaks persist deep into the antinodal region. Temperature dependence shows that the gap along much of the Fermi surface ($75° > \theta > 15°$) vanishes above T_c. But surprisingly, the antinodal gap survives above T_c with a similar gap magnitude but without coherence peaks and eventually vanishes between 80 and 100 K [Fig. 2(c)], indicating a persisting pseudogap in the overdoped region of 2201, consistent with a prior study on overdoped Pb-Bi2201 samples [16]. Correspondingly, our STM data reveal two spatially coexisting gaps [Figs. 1(e) and 1(g)] confirming the presence of the pseudogap below T_c. Comparing the STM and ARPES gaps below T_c for 0.1La, we find that the average small gap (7 ± 2 meV) is comparable to the antinodal ARPES gap ($\sim$8 meV). Thus for both dopings the average STM small gap can be identified with the superconducting order parameter and scales as expected with T_c.

Having identified Δ_s with superconductivity, what can we say about the origin of the large gap, Δ_L? There are many conjectures for the pseudogap state in hole-doped cuprates ranging from static order to fluctuating order of density waves in the particle-particle or the particle-hole channels. Charge ordering in the form of short-range ordered checkerboard patterns has previously been observed in other compounds by STM both below T_c [17–19] and above T_c [19,20]. To explore this possibility we obtain Fourier transforms of dI/dV maps at various energies. On the 0.4La samples, a glassy form of charge order is revealed as shown in Fig. 3(a). The corresponding wave vector (q vector) observed in the Fourier transform is $2\pi/(5 \pm 1)a_0$ in the $(0, \pm\pi)$ direction [Fig. 3(c)] and is nondispersing with energy. The STM q vector matches well with the vector connecting the Fermi arc tip observed in our ARPES data which is $2\pi/(5.2 \pm 0.7)a_0$ [Fig. 3(e)]. While the nondispersive nature of the ordering rules out the possibility of quasiparticle interference, can this charge order be classified as a bona fide charge density wave (CDW) that can result in a CDW gap? An important signature of CDW in the local density of states is contrast reversal [21]. Similar to previous STM data, we find no evidence for contrast reversal at low energies (<15 meV) [22]. But at higher energies (± 50 meV), we observe ubiquitous signals for contrast reversal as exemplified in Fig. 4(a). The coherence length for the CDW pattern is rather short $\sim$10–15 Å which would make it difficult to observe using scattering probes.

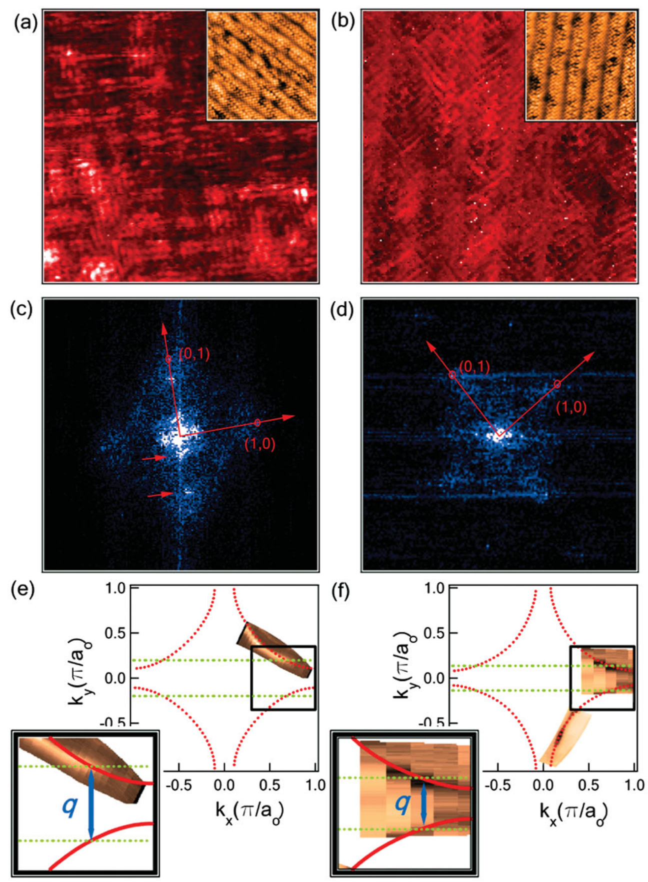

FIG. 3 (color). (a) 160 Å dI/dV map [$g(r, E)$] of 0.4La sample at energy $(E) = +7$ meV. Inset shows simultaneous topography. (b) 160 Å $g(r, E)$ map of 0.1La sample at $E = -11$ meV. (c) Fourier transform of map in (a) showing the q vectors arising from the CDW pattern. The unit for the axis is $2\pi/a_0$ where lattice constant $a_0 = 3.83$ Å. (d) Fourier transform of map in (b). (e) ARPES Fermi surface mapping of 0.4La sample. The inset shows the nesting vector at the arc tip which matches the average STM periodicity. (f) ARPES Fermi surface mapping of 0.1La sample showing the now smaller q vector.

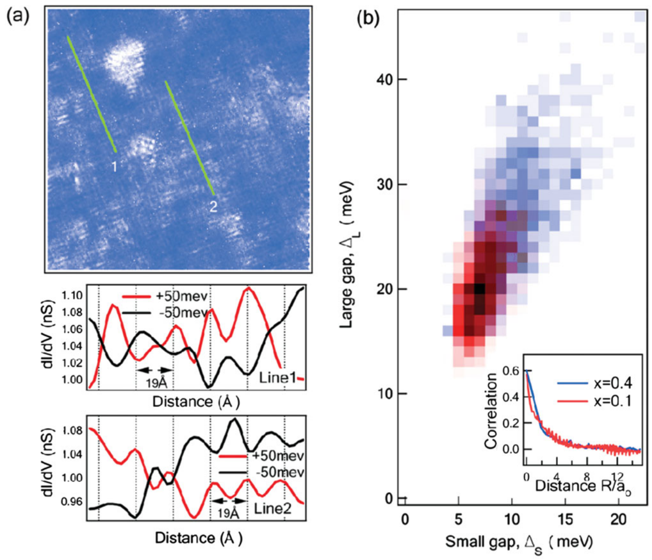

FIG. 4 (color). (a) 237 Å $g(r, E)$ map at $E = 0$ meV, showing the position of the two line cuts used to illustrate contrast reversal. Shown below the map, are smoothed linecuts from simultaneously obtained maps at $E = +50$ meV and -50 meV. (b) Scatter plot of occurrences of Δ_s and Δ_L for the data plotted in Fig. 1(c) (0.4La, blue squares) and Fig. 1(g) (0.1La, red squares). The inset shows the spatial dependence of the cross correlation between the Δ_s and Δ_L maps which retains a finite value up to a few lattice constants.

In the overdoped 0.1La samples, the vector connecting the arc tip observed by ARPES ($q \approx 2\pi/(7 \pm 0.5)a_0$) is expected to result in a spatial ordering with periodicity ~27 Å [Fig. 3(f)]. Since the CDW displays short-range coherence, this larger periodicity is not likely to be sustainable. More importantly, the kinetic motion of the increasing number of doped holes is enhanced in the overdoped samples. Correspondingly, we find no clear CDW pattern at this doping [Figs. 3(b) and 3(d)] and the large gap is suppressed in magnitude [Figs. 1(e) and 1(g)]. The concomitant suppression of the large gap and the CDW pattern suggests an intimate connection between the two, even implying a likely causal relationship. The weak pseudogap in the overdoped samples could potentially arise either from CDW fluctuations or a static CDW that is too weak or disordered to be observed by STM.

Finally, CDW ordering is just one amongst many explanations for this pseudogap and while we cannot entirely rule out the possibility that the occurrence of the CDW is coincidental or a surface phenomenon, we can certainly comment on an orthogonal explanation, i.e., the fluctuating pair origin of this pseudogap. Based on our data it would be difficult to reconcile our observations of two coexisting gaps below T_c in real space and momentum space, with the assumption that the observed large pseudogap is caused by fluctuating (precursor) pairs. We would like to stress however, that our data do not rule out the possibility of an additional smaller pseudogap related to pair fluctuation existing for a narrow temperature range above T_c.

An important observation in the STM data is that there is a strong correlation between the small and the large gaps. Figure 1(h) shows STM spectra on 0.4La samples that were sorted and averaged based on Δ_L. One can clearly see that as the large-gap increases, so does the magnitude of the small gap. This is also true statistically as seen by the scatter plot in Fig. 4(b). The cross correlation between the two gaps gives a rather strong correlation onsite coefficient of 0.6 indicating that both order parameters are influenced by the same underlying physical processes. A key point to note here is that while the second larger gap in the 0.1La samples is rather weak and not always observed, wherever it is visible it shows the same correlation with the superconducting gap as the 0.4La sample [Fig. 4(b)]. Furthermore, the seamless continuation of the scatter plot for the 0.1La samples with the 0.4La samples suggests that the gap variations for both gaps may arise from doping inhomogeneities [23–25].

In summary, the STM and ARPES data reveal critical new information about the pseudogap phase in Bi2201. First, unlike Bi2212, the pseudogap and Fermi arc above T_c extend into the overdoped regime. Second, in Bi2201, a pseudogap above T_c is accompanied by two gaps below T_c that coexist in real space and in momentum space, leading us towards a competing order explanation for this elusive phase.

We thank E. W. Hudson and Tanmoy Das for helpful discussions. This work was supported in part by grants from the NSF.

[1] H. Ding *et al.*, Nature (London) **382**, 51 (1996).
[2] A. G. Loeser *et al.*, Science **273**, 325 (1996).
[3] T. Timusk and B. Statt, Rep. Prog. Phys. **62**, 61 (1999).
[4] M. Shi *et al.*, Phys. Rev. Lett. **101**, 047002 (2008).
[5] K. Tanaka *et al.*, Science **314**, 1910 (2006).
[6] T. Kondo *et al.*, Phys. Rev. Lett. **98**, 267004 (2007).
[7] S. Hufner *et al.*, Rep. Prog. Phys. **71**, 062501 (2008).
[8] M. Le Tacon *et al.*, Nature Phys. **2**, 537 (2006).
[9] W. S. Lee *et al.*, Nature (London) **450**, 81 (2007).
[10] F. C. Niestemski *et al.*, Nature (London) **450**, 1058 (2007).
[11] S. Souma *et al.*, Rev. Sci. Instrum. **78**, 123104 (2007).
[12] J. Wei *et al.*, Phys. Rev. Lett. **101**, 097005 (2008).
[13] M. Civelli *et al.*, Phys. Rev. Lett. **100**, 046402 (2008).
[14] Tanmoy Das *et al.*, Phys. Rev. B **77**, 134516 (2008).
[15] L. Ren and Z. Wang, arXiv:0807.4531.
[16] M. C. Boyer *et al.*, Nature Phys. **3**, 802 (2007).
[17] Y. Kohsaka *et al.*, Science **315**, 1380 (2007).
[18] T. Hanaguri *et al.*, Nature (London) **430**, 1001 (2004).
[19] W. D. Wise *et al.*, Nature Phys. **4**, 696 (2008).
[20] M. Vershinin *et al.*, Science **303**, 1995 (2004).
[21] G. Gruner and A. Zettl, Phys. Rep. **119**, 117 (1985).
[22] T. Hanaguri *et al.*, Nature Phys. **3**, 865 (2007).
[23] S. H. Pan *et al.*, Nature (London) **413**, 282 (2001).
[24] Ziqiang Wang *et al.*, Phys. Rev. B **65**, 064509 (2002).
[25] Sen Zhou *et al.*, Phys. Rev. Lett. **98**, 076401 (2007).